Demons and superconductivity

J. Ihm* and Marvin L. Cohen
Department of Physics, University of California and Materials and Molecular Research Division, Lawrence Berkeley Laboratory, Berkeley, California 94720

S. F. Tuan
Department of Physics and Astronomy, University of Hawaii, Honolulu, Hawaii 96822
(Received 22 October 1980)

Model calculations are used to explore the role of demons (acoustic plasmons involving light and heavy mass carriers) in superconductivity. Heavy *d* electrons and light *s* and *p* electrons in a transition metal are used for discussion, but the calculation presented is more general, and the results can be applied to other systems. The analysis is based on the dielectric-function approach and the Bardeen-Cooper-Schrieffer theory. The dielectric function includes intraband and interband *s*-*d* scattering, and a tight-binding model is used to examine the role of *s*-*d* hybridization. The demon contribution generally reduces the Coulomb interaction between the electrons. Under suitable conditions, the model calculations indicate that the electron-electron interaction via demons can be attractive, but the results also suggest that this mechanism is probably not dominant in transition metals and transition-metal compounds. An attractive interband contribution is found, and it is proposed that this effect may lead to pairing in suitable systems.

I. INTRODUCTION

It is well known that plasmas consisting of constituents with differing masses exhibit soundlike normal modes. In solids, one standard example of this phenomenon is the existence of acoustic phonons in a system containing ions and electrons. The ionic plasma frequency is screened by the dielectric function appropriate to the electrons, and the resulting acoustic mode (frequency linear in wave vector) is a sound mode of the system. Other examples include heavy holes screened by light electrons and heavy electrons of one type screened by light electrons of another variety. These modes are acoustic plasmons.

Electron-electron interactions can be affected by the existence of modes of this type. In analogy with phonon exchange, soundlike modes can reduce the Coulomb repulsion between electrons, or they can cause an attractive interaction between electrons. There are other similar pairing mechanisms like electron-hole couplings[1-4] which have been of recent interest. This paper will focus on the heavy–light-mass-electron case. For simplicity, we will refer to the light-mass electrons as *s* electrons and the heavy-mass electrons as *d* electrons; however, the calculation is more general and the results are applicable to most two-carrier systems.

In 1955, Pines[5] explored the existence of acoustic plasmonlike modes focusing primarily on the semiconductor case. He associated the term *demon* or *d-mon* with "distinct electron motion or D.E.M." In the present paper, we will use this term to refer to d-electron acoustic plasmons. Garland[6] proposed the application of the *s*-*d* electron interaction to couple electrons for superconductivity in transition metals. Later, Radhakrishnan,[7] Fröhlich,[8] and Rothwart[9] investigated the mechanism further, and Ganguly and Wood[10] examined the possible influence of acoustic plasmons on phonon dispersion curves. Following Kleiwer *et al.*[11] lifetime effects were included by some of these authors using a phenomenological scattering time. More recently, Ruvalds and collaborators[12] reinvestigated the demon model and focused on the possible influence of this mechanism on superconductivity in transition metals and compounds.

Most of the above calculations concluded that acoustic plasmons in solids should exist. However, to our knowledge, their existence has not been verified convincingly by experiment. A possible reason for this could be the significant lifetime effects[11] which can overdamp these modes. For the demon case itself, most of the theoretical estimates conclude that an attractive electron-electron interaction can result from the exchange of demons; however, several objections to this mechanism have been proposed. Garland[13] has suggested that (*s*-*p* electron) $-$(*d* electron) scattering will average these states be-

fore the pairing interaction is effective. This scattering will blur the distinction between *s-p* and *d* electrons, and the antiscreening effects expected from the *d* electrons will be reduced or eliminated. In addition, this scattering will average the superconducting gaps[14] causing further reduction.

Another source for the lack of motivation for research on the demon mechanism is the fact that previous authors focused on transition metals, and the electron-phonon description of *d*-band metal superconductivity has been very successful in explaining many of the observed superconductive properties of these materials[15,16] without including demon effects.

Despite these objections and concerns, we have reinvestigated this problem to attempt to answer some of the theoretical questions surrounding the mechanism itself. In principle, impurity scattering in *d*-band materials can be reduced, and the question remains as to whether the properties of pure materials (not only transition metals) can be influenced by acoustic plasmons. The hybridization of the *s-p* and *d* bands is an intrinsic effect, and this contribution requires investigation. The calculation presented here examines hybridization, and the complex dielectric functions are calculated over the *entire* (q, ω) plane. Another important feature of the present calculation is the consideration of interband scattering in the dielectric function, $\epsilon(q, \omega)$. Interband scattering is found to reduce the influence of the acoustic plasmon, but we find that the interband scattering itself gives rise to new additional attractive contributions. Finally, even if the prognosis for demon superconductivity is not bright for transition metals, our calculation also encompasses other multiple-carrier systems, and we hope to motivate research on other materials.

II. CALCULATIONS

The superconductivity aspects of this calculation are based on the BCS theory.[17] The electron-electron interaction is evaluated using a dielectric-function formalism. Contributions beyond the random-phase approximation (RPA) are ignored, and the dielectric functions are calculated using the standard self-consistent-field approach.[18]

A. Intraband contribution to $\epsilon(q, \omega)$

To estimate the effect on superconductivity of the Coulomb interaction for two partly filled bands, we begin by taking the extreme model of a free-electron dielectric function including contributions from both *s* and *d* electrons. (Some of the results of this calculation were reported previously.[3]) Interband terms are not included in the dielectric function at this stage; they will be added later and discussed separately. The effects of *s-d* hybridization will also be taken into account in a later section using a tight-binding model.

These simplifications yield a dielectric function

$$\epsilon(q, \omega) = 1 + \pi_s + \pi_d, \tag{1}$$

where π is the polarization for each type of electron. We have not distinguished between purely *s* and mixed *s-p* bands. The calculation is similar for both cases. π is expressed in the self-consistent-field approximation[18] as

$$\pi(q, \omega) = -\frac{4\pi e^2}{\Omega q^2} \sum_k \frac{f_{k+q} - f_k}{E_{k+q} - E_k - \hbar\omega - i\eta}. \tag{2}$$

The summation is over the *s* band or the *d* band. The effective masses (m_s and m_d) and the Fermi wave vectors (k_F^s and k_F^d) are input parameters and Ω is the crystal volume. We choose $m_s = m_e$, the free-electron mass, and $k_F^s = 0.5 a_B^{-1}$ where a_B is the Bohr radius. The calculations are done for various values of m_d/m_s and k_F^d/k_F^s.

The dielectric function with *s* electrons alone is the standard Lindhard[19] dielectric function which has a negative region in the (q, ω) plane. This attractive region lies in the small-q portion of the plane, that is,

$$\epsilon_1 < 0, \quad \text{if } \tfrac{5}{6} v_F^s q \lesssim \omega \lesssim \omega_{pl}^s(q), \tag{3}$$

where ϵ_1 is the real part of ϵ, v_F^s is the Fermi velocity of *s*-electrons, and ω_{pl}^s is the *s*-electron plasma frequency. The $\epsilon_1 < 0$ region is illustrated in Fig. 1. For the *d*-electrons alone, $(1 + \pi_d)$ is also shown in the same figure to scale. The values $m_d/m_s = 10$ and $k_F^d/k_F^s = 1$ were chosen. The two contributions are added together $(1 + \pi_s + \pi_d)$, and the real part of the total ϵ is shown in Fig. 2. From the total dielectric function, we can evaluate the Coulomb kernel K_c to be used in the superconducting gap equation[17]

$$D_k = -\tfrac{1}{2} \int \frac{D_{k'}}{E_{k'}} (K_p + K_c) \tanh \frac{E_{k'}}{2kT} d\epsilon_{k'}, \tag{4}$$

where the sum of K_p and K_c, the phonon and Coulomb kernels of the gap equation, is a measure of the BCS "$N(O)V$" parameter. The energy gap Δ_k is normalized $[D_k = (k/k_F^s)\Delta_k]$ for convenience. We will focus on the Coulomb kernel[20] which can be evaluated from the dielectric function

$$K_c = \left(\frac{4}{9\pi^4}\right)^{1/3} r_s \frac{k_F}{k'} \int_{|\vec{k}-\vec{k}'|}^{|\vec{k}+\vec{k}'|} \mathrm{Re}\left[\frac{1}{\epsilon(q, \omega)}\right] \frac{dq}{q}. \tag{5}$$

The region of integration (Figs. 1 and 2) is over the momentum conservation or Landau damping region for the electrons under consideration (*s* or *d*). There is an attractive contribution to K_c when $\epsilon_1 < 0$.

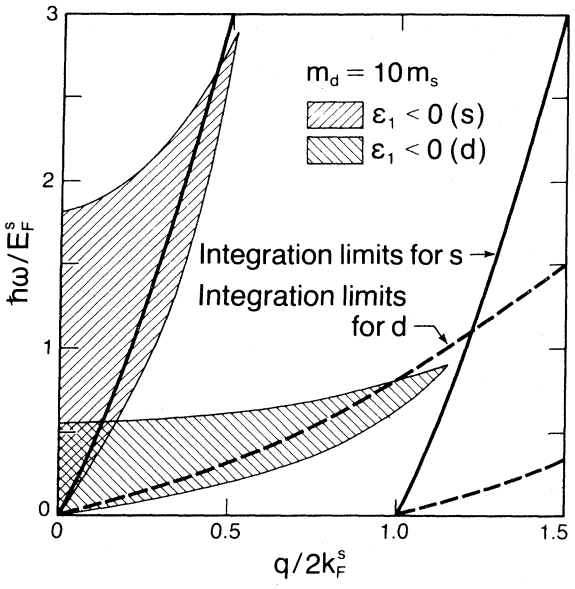

FIG. 1. Properties of the Lindhard dielectric function shown in the (q, ω) plane. The shaded regions represent $\epsilon_1 < 0$ for s electrons or for d electrons. The parameters are: m_s is the free-electron mass, $k_F^s = k_F^d = 0.95 \times 10^8$ cm^{-1}, and $E_F^s = 3.4$ eV. The solid and dashed lines denote the integration limits of q for calculating the Coulomb kernel, $K_c(\omega)$, of s and d electrons, respectively. They coincide with the region defining $\epsilon_2 \neq 0$.

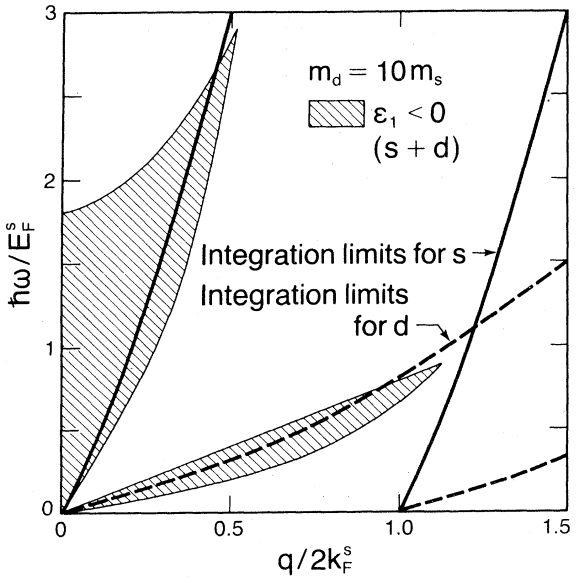

FIG. 2. The dielectric function of the combined s- and d-electron system without interband scattering [Eq. (1)] is shown in the (q, ω) plane. Parameters are the same as in Fig. 1.

If the s or d electrons are treated separately, the corresponding K_c is repulsive since the overlap of the region of integration with the $\epsilon_1 < 0$ region is small (see Fig. 1). However, in the combined case (Fig. 2), the d-plasma frequency is renormalized to produce the demon mode which is the new upper bound on the attractive region associated with the d electrons. The lower bound of this region remains $\omega \cong \frac{5}{6} v_F^d = \frac{5}{6}(m_s/m_d) v_F^s q$ for small q. The integral range for the Coulomb kernel of s electrons now includes the attractive region induced by demon modes. This region of attractive interaction is determined by m_d/m_s and k_F^d/k_F^s. The demon dispersion relation

$$\omega = \alpha v_F^s q \tag{6}$$

for small q can be calculated numerically. In particular, if $k_F^d = k_F^s$ and $m_d/m_s = l$, α is the solution of the following simple equation:

$$2 + \alpha \ln\left|\frac{1-\alpha}{1+\alpha}\right| + l\left(2 + l\alpha \ln\left|\frac{1-l\alpha}{1+l\alpha}\right|\right) = 0. \tag{7}$$

Three real, distinct solutions exist if $l > 2.26$, and the intermediate solution corresponds to the demon mode. If $l \gg 1$ and $k_F^d/k_F^s = \gamma$, it is easy to show that the dispersion relation approaches

$$\omega = \left(\frac{\gamma}{3l}\right)^{1/2} v_F^s q. \tag{8}$$

For a fixed value of γ, the d-attractive region moves down to a lower frequency as l increases. When integrated over the Landau damping region of q, $K_c(\omega)$ for s electrons is reduced at low ω because of the attractive d contributions. This trend is shown in Fig. 3. Assuming $\gamma = 1$, K_c is significantly reduced at low ω for $l = 5$. For larger mass ratios ($l = 10$), K_c is still reduced at low ω, but it is relatively unchanged from the s-only results at higher ω. For very large ratios, that is, $l \gtrsim 20$, the kernel becomes negative at very small positive ω. For $\omega = 0$, K_c is always positive but reduced in magnitude because of the larger screening from the d electrons. In the Thomas-Fermi model,[2] $K_c(\omega{=}0) = \frac{1}{2}(r_s/a)\ln(1 + a/r_s)$ where $a = (\frac{9}{4}\pi^4)^{1/3} \cong 6$, $r_s = a/\pi a_B k_F$, and $a_B = \hbar^2/m^* e^2$. If we have s and d electrons, the same model for large mass ratios (i.e., for $r_s^s << r_s^d$) gives

$$K_c(\omega{=}0) \cong \frac{1}{2}\frac{r_s^s}{a}\ln\left(1 + \frac{a}{r_s^d}\right) . \tag{9}$$

Hence, the major effect of the demons is to reduce K_c at low ω enhancing the effects of the attractive phonon interaction if this conventional superconducting mechanism is present.

At very large m_d/m_s, K_c can become attractive, but the free-electron model which we are using can become inappropriate in this limit. We have also stud-

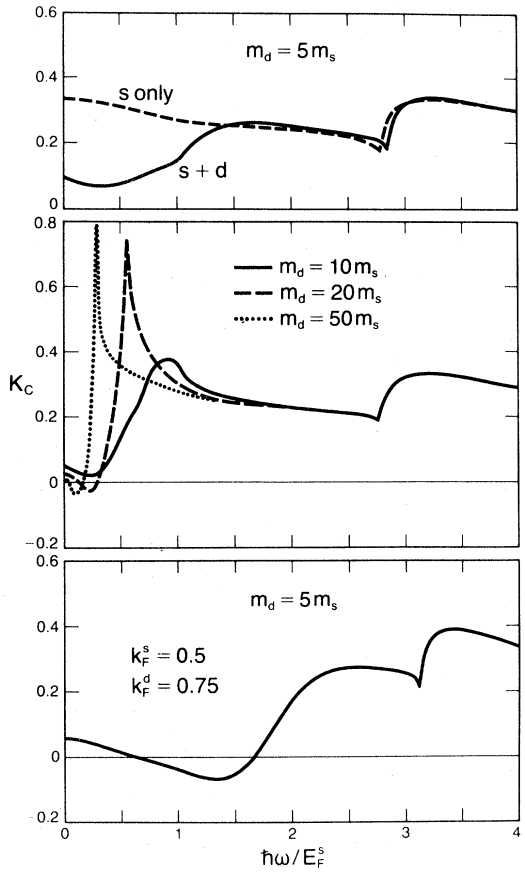

FIG. 3. The Coulomb kernel $K_c(\omega)$ entering the superconducting gap [Eq. (4)] for s electrons. The top figure shows the $K_c(\omega)$ calculated from the Lindhard dielectric function for s electrons (dashed lines) and for the combined s- and d-electron systems (solid lines). Two ratios of k_F^d/k_F^s are considered. The central figure illustrates the $K_c(\omega)$ of the combined s and d electrons with different mass ratios. The bottom figure displays the $K_c(\omega)$ with $k_F^s = 0.5$ and $k_F^d = 0.75$.

ied the effect of variable γ. In general, the reduction of the Coulomb interaction becomes larger as γ becomes larger; that is, there is more d-electron screening of the interaction of the s-electron pair. The result with $k_F^s = 0.5$, $k_F^d = 0.75$, and $l = 5$ is presented in Fig. 3 which shows an attractive interaction region. Although the above calculations include damping arising from the electron-hole continuum (i.e., we have considered ϵ_2 in calculating the real part of $1/\epsilon$), the influence of scattering by impurities, phonons, or defects is not taken into account. These latter effects would average the s and d electrons and the superconducting gaps as discussed previously.

The evaluation of the K_c for d electrons involves a different region of integration in the (q, ω) plane (Figs. 1 and 2). The result is shown in Fig. 4. The

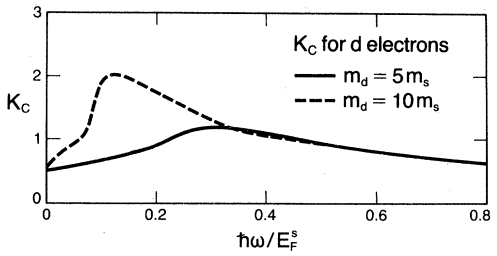

FIG. 4. The Coulomb kernel $K_c(\omega)$ entering the superconducting gap [Eq. (4)] for d electrons.

Coulomb kernel for the d electrons is not affected significantly by the presence of s electrons.

B. Interband scattering correction

In this case, we repeat the calculation of K_c, but we now include the s-d interband contributions to ϵ. Using the self-consistent-field dielectric function,[18] we now have

$$\epsilon = 1 + \pi_s + \pi_d + \pi_{sd} \ , \tag{10}$$

$$\pi_{sd} = -\frac{4\pi e^2}{\Omega q^2} \sum_k \left\{ \frac{(f_{k+q,s} - f_{k,d})|M_{ds}|^2}{E_{k+q,s} - E_{k,d} - \hbar\omega - i\eta} + \frac{(f_{k+q,d} - f_{k,s})|M_{sd}|^2}{E_{k+q,d} - E_{k,s} - \hbar\omega - i\eta} \right\} , \tag{11}$$

$$M_{ds} = \langle k,d|e^{-i\vec{q}\cdot\vec{r}}|k+q,s\rangle = \int u_{k,d}^* u_{k+q,s} d^3r \ , \tag{12}$$

where f is the occupation number and u is the cell-periodic part of the Bloch function. The matrix element M is unity in the free-electron model. This is a reasonable approximation for the intraband transition but not for interband scattering. For example, M should be exactly zero between (k,n) and (k',n') states if $k' = k$ and $n' \neq n$ from the orthogonality of wave functions. For general interband scattering $(k' \neq k,\ n' \neq n)$, M is nonzero but much smaller than 1 if the scattering is between s and d states where the character of the wave functions changes very significantly. This case will be treated accurately in the next section using the tight-binding model. In the present free-electron model, we regard the $|M|^2$'s as parameters and study the effect of the interband terms for various values of $|M|^2$.

To illustrate the influence of interband scattering, we choose $k_F^d = k_F^s = 0.5$, $m_d/m_s = 10$, and $|M|^2 = 1$. By suitable relabeling of indices in Eq. (11), we have

$$\pi_{sd}=\frac{4\pi e^2}{\Omega q^2}\sum_k\left[\frac{f_{k,s}}{E_{k+q,d}-E_{k,s}-(\hbar\omega+i\eta)}+\frac{f_{k,s}}{E_{k+q,d}-E_{k,s}+(\hbar\omega+i\eta)}\right.$$
$$\left.+\frac{f_{k,d}}{E_{k+q,s}-E_{k,d}-(\hbar\omega+i\eta)}+\frac{f_{k,d}}{E_{k+q,s}-E_{k,d}+(\hbar\omega+i\eta)}\right]\equiv A+B+C+D\ . \tag{13}$$

A, B, C, and D represent four different transitions contributing to π_{sd}. These terms will be studied separately although there are partial cancellations among them. Details of each term depend on the particular choices of k_F^s, k_F^d, m_s, and m_d; however, some characteristic features of each term are quite general irrespective of the parameters. Only the results with $k_F^s=k_F^d$ will be described below.

The interband term, π_{sd}, is decomposed into A, B, C, and D contributions as shown in Fig. 5. For brevity, let A, B, C, and D denote the real parts of the respective terms. A is basically negative above a frequency ω_c which is approximately the difference between the average energy of the d band and the occupied s band. This behavior is easily seen to come from the $-\hbar\omega$ term in the denominator of Eq. (13). B is positive for positive ω if $k_F^d=k_F^s$ because $(E_{k+q,d}-E_{k,s})$ is almost always positive whenever $f_{k,s}\neq 0$. This property depends somewhat on the relative lineup of the s and d bands. C has negative contributions from the region

$$\hbar\omega\geq E_{k+q,s}-E_{k,d}=\frac{\hbar^2}{2}\left[\frac{q^2}{m_s}+\frac{2kq}{m_s}+\left(\frac{k^2}{m_s}-\frac{k^2}{m_d}\right)-\left(\frac{k_F^{s2}}{m_s}-\frac{k^2-k_F^{d2}}{m_d}\right)\right]\ . \tag{14}$$

After integrating over k, we find the approximate condition

$$C\lesssim 0,\ \text{if}\ \hbar\omega\gtrsim\frac{\hbar^2q^2}{2m_s}+\frac{\hbar^2q\langle k\rangle}{m_s}-\text{const}\ , \tag{15}$$

where $\langle k\rangle$ represents a weighted average of k ($\sim$ order of k_F^d). The above argument explains the behavior of C in Fig. 5. D is essentially positive except for a small (q,ω) region for the same reason as in the case of B.

The sum of four contributions, which is rather structureless, is shown on the same figure. With this contribution added to the previous intraband terms, the negative region of the real part of the total dielectric function [Eq. (10)] is shown in Fig. 6. The negative contribution of the demon mode is significantly reduced but still exists, and the interband scattering gives rise to an additional attractive branch around $\hbar\omega\approx E_F^s$. This is mainly due to the negative contribution for A. Figure 7 shows the Coulomb kernel screened by this total dielectric function. Major changes occur for intermediate ranges of ω,

$$0.3E_F^s\lesssim\hbar\omega\lesssim 2E_F^s\ . \tag{16}$$

Up to this point, the variation in $|M|^2$ has not been included in the calculation. We attempted to estimate $|M|^2$ between Bloch states formed by atomic s orbitals and atomic d orbitals. The calculated values for $|M|^2$ are much smaller than unity indicating that the results without interband contributions (Figs. 2, 3, and 4) are closer to the actual situation than the results of this section (Figs. 6 and 7) where interband contributions are exaggerated.

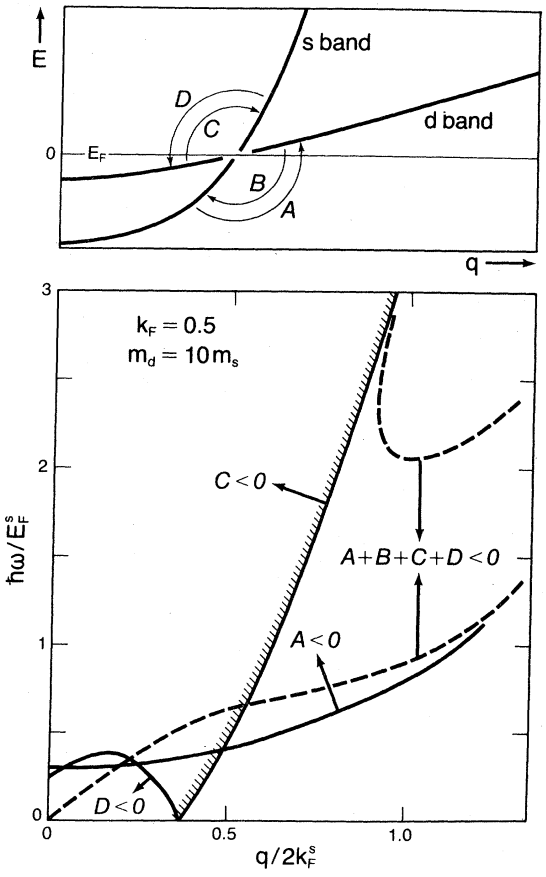

FIG. 5. Four contributions to π_{sd} [Eq. (13)]. A, B, C, and D represent the four transitions shown. The region where the real part of each contribution is negative is marked. B is always positive in this case ($k_F^s=k_F^d=0.5$ and $m_d=10m_s$). The negative region for the sum of the four contributions is also shown.

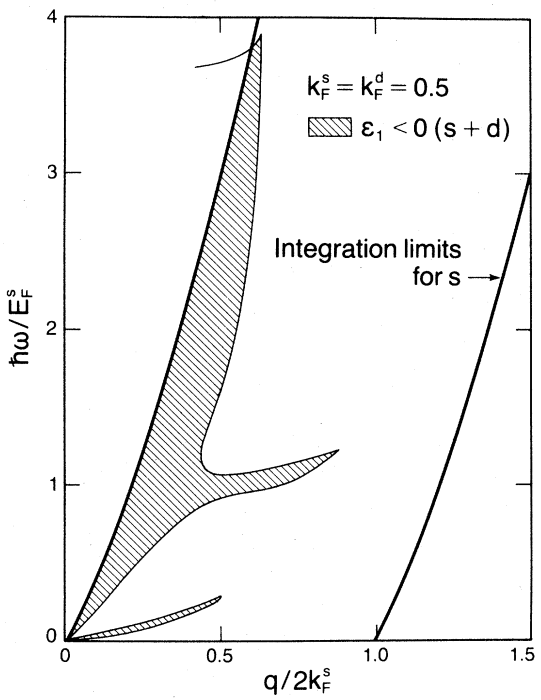

FIG. 6. The dielectric function of the combined s and d electrons including interband scattering is shown in the (q, ω) plane. The range for $\epsilon_1 < 0$ within the Landau damping region is shaded. The matrix element $|M|^2$ is artificially assumed to be unity to emphasize the effects of the interband terms. For realistic models, $|M|^2 << 1$.

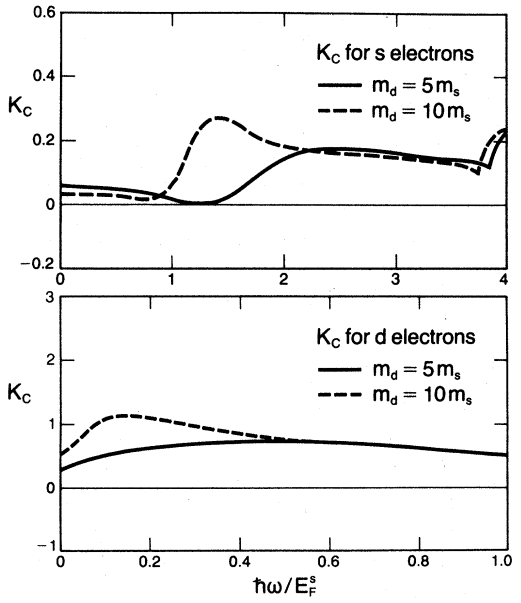

FIG. 7. The Coulomb kernel $k_c(\omega)$ for s electrons and for d electrons including the interband contribution with $|M|^2 = 1$.

However, if hybridization of s and d electrons occurs, two changes can occur which are not treated properly in the model used. The interband matrix elements can become larger, and the two bands do not cross. Off-diagonal matrix elements may significantly alter the small-ω region ($\hbar\omega \lesssim E_{\text{splitting}}$). In the next section, we include hybridization and the matrix-element effects in the calculation.

C. Hybridization

To consider the hybridization of s and d electrons, it is convenient to work within the tight-binding model. For simplicity, a simple cubic structure is assumed with only nearest-neighbor interactions. Two half-filled bands, s and d, are assumed, and using the standard tight-binding approach, we get the determinant equation

$$\begin{vmatrix} \epsilon - (\epsilon_s - \beta_{ss} - \tilde{\gamma}_{ss}) & \beta_{sd} + \tilde{\gamma}_{sd} \\ \beta_{ds} + \tilde{\gamma}_{ds} & \epsilon - (\epsilon_d - \beta_{dd} - \tilde{\gamma}_{dd}) \end{vmatrix} = 0 \ , \tag{17}$$

where

$$\epsilon_i = \text{term value of the } i\text{th atomic orbital}, \tag{18}$$

$$\tilde{\gamma}_{ij}(k) = 2\gamma_{ij}(R)(\cos k_x R + \cos k_y R + \cos k_z R) \ , \tag{19}$$

$$\gamma_{ij}(R) = -\int \phi_i^*(r)\Delta u(r)\phi_j(r-R)d^3r \ , \tag{20}$$

$$\beta_{ij} = \gamma_{ij}(R=0) \ . \tag{21}$$

ϕ_i is the ith atomic orbital, $\Delta u(r)$ is the difference between the crystal potential and the atomic potential, and R is the nearest-neighbor distance. We vary the above parameters to observe the change in $\epsilon(q, \omega)$, but in the results presented below, we have assumed $R = 5a_B = 2.65$ Å, $\gamma_{ss} = 0.05$ Ry, $\gamma_{dd} = 0.01$ Ry, $\gamma_{sd} = \gamma_{ds} = 0.004$ Ry, $\beta_{sd} = \beta_{ds} = 0.012$ Ry, and $\epsilon_s - \beta_{ss} = \epsilon_d - \beta_{dd} = 0$. The band structure in an arbitrary direction of $\vec{k}$ is sketched in Fig. 8. The Fermi energy is ~ 0.3 Ry, and the total density of electrons is $\sim 10^{23}/\text{cm}^3$. Since the band structure is not isotropic, we need to choose a specific direction for q; we have chosen $\epsilon(q_x, \omega)$. The calculation of ϵ involves a straightforward numerical integration.

In the $q \to 0$ limit, the properties of ϵ in the two-band model can be studied analytically. The intraband contribution is described accurately using the optical-plasmon frequencies ω_{pl}^s and ω_{pl}^d,

$$\pi_s + \pi_d = -\frac{\omega_{\text{pl}}^{s2}}{\omega^2} - \frac{\omega_{\text{pl}}^{d2}}{\omega^2} \ . \tag{22}$$

Interband contribution comes only from that part of the Brillouin zone where the lower band is filled and the upper band is empty. The difference in energy ($E_{\text{upper}} - E_{\text{lower}}$) is more or less constant in this re-

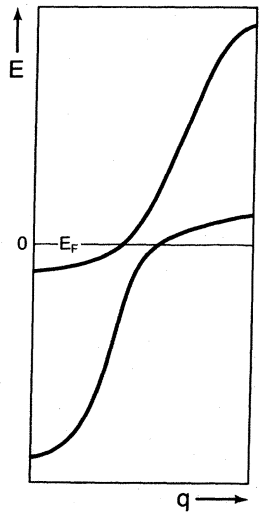

FIG. 8. A schematic band structure of hybridized s and d bands in an arbitrary direction of $\vec{k}$.

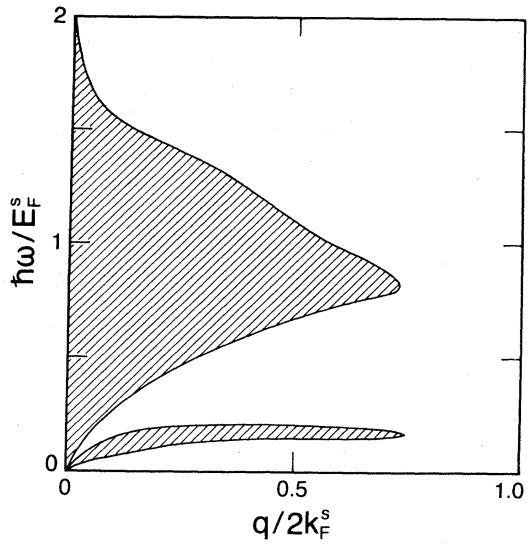

FIG. 9. The self-consistent field dielectric function of combined s and d electrons in the tight-binding model described in the text. The region of $\epsilon_1 < 0$ is shown shaded in the (q_x, ω) plane.

gion and equal to the average band splitting $E_{\text{split}} \approx 2\beta_{sd}$. The interband term is then

$$\pi_{sd} \cong \frac{\omega_{\text{pl}}^{*2}}{(E_{\text{split}}/\hbar)^2 - \omega^2} , \tag{23}$$

where ω_{pl}^{*} is a constant corresponding to a plasma frequency arising from the interband interaction. The final expression is

$$\epsilon(0, \omega) \cong 1 - \frac{\omega_{\text{pl}}^{s\,2} + \omega_{\text{pl}}^{d\,2}}{\omega^2} + \frac{\omega_{\text{pl}}^{*2}}{(E_{\text{split}}/\hbar)^2 - \omega^2} . \tag{24}$$

For nonzero q, the calculation is done numerically using the self-consistent-field dielectric function. The result is shown in Fig. 9. The demon mode again exists here even though the present tight-binding model is completely different from the previous free-electron model. The shape of the upper negative (s-plasmon) region is somewhat changed because of matrix-element effects, interband scattering, and the finite width of the bands. Since the present section only aims at supplementing the previous results and the details depend on the input parameters, we did not calculate $K_c(\omega)$ for this model. We just note that the qualitative features of $\epsilon(q, \omega)$ are the same as they were before, and the reduction of $K_c(\omega)$ for small ω is significant in both models.

D. Paramagnon effects

The effects of spin fluctuations (paramagnons) on the superconductivity are considered here. This effect was studied by several authors[21–24] primarily to understand why materials of high susceptibility (χ) like Pd do not exhibit superconductivity. The basic argument was that the Coulomb repulsion is enhanced for singlet spin pairing because of ferromagnetic spin polarizations induced by interacting electrons. An up-spin electron A will induce electrons of up-spin around it. The partner electron B with down-spin, attempting to lower its energy by taking advantage of the phonon attraction produced by A in the usual singlet BCS picture, must first pass through a region of unfavorably oriented spins. Thus, there is an effective Coulomb repulsion originating from spin fluctuations. This effect was calculated as a function of μ,[22] and it was found to be small compared with μ except for high-χ materials like Pd.

Still, it is interesting to note that a very close relationship exists between $\epsilon(q, \omega)$ and $\chi(q, \omega)$. For paramagnetic materials, the wave-vector and frequency-dependent susceptibility per atom is written[25]

$$\chi(q, \omega) = \frac{\Gamma(q, \omega)}{1 - U\Gamma(q, \omega)} , \tag{25}$$

$$\Gamma(q, \omega) = -\frac{1}{N} \sum_k \frac{f_{k+q} - f_k}{E_{k+q} - E_k - \hbar\omega - i\eta} . \tag{26}$$

U is the positive exchange interaction parameter, and $\Gamma(q, \omega)$ is the same response function as that used in the calculation of the dielectric function, Eq. (2). The denominator $(1 - U\Gamma)$ in Eq. (25) is always positive for paramagnetic materials. If $\text{Re}\epsilon(q, \omega) < 0$ for a certain region of (q, ω), then $\chi(q, \omega)$ is also negative. Thus, although $\chi(0, 0)$ is always positive for paramagnetic materials, $\chi(q, \omega)$ can be negative

which in turn means it will lead to an attractive interaction. In particular, the attractive interaction from negative χ can be effective, though not large, in enhancing T_c because it usually occurs when $\epsilon < 0$. The physical origin of the negative χ is the same as for negative ϵ. The overscreening by d plasmons induces opposite-spin electrons around a given electron in contrast to the usual static paramagnetic case. Negative regions of $\chi(q, \omega)$ are broader in the (q, ω) plane than that of $\epsilon(q, \omega)$ as χ does not include a constant 1 in its definition. There is repulsion for the positive-χ region. The exchange term in Eq. (25) enhances the repulsion and reduces the attraction, but this is still one order of magnitude smaller. Because the exchange parameter U is not known, we will not try to evaluate the magnitude of the contribution from spin fluctuations. It can be included as a correction in K_c.

III. CONCLUSIONS

We have shown that the interaction of s and d electrons can reduce the effective Coulomb repulsion in important regions of the (q, ω) plane and enhance T_c. Two mechanisms are considered—demons and interband scattering. The demon mechanism is reduced but not eliminated by interband scattering. The interband scattering itself provides an attractive contribution in the high-frequency regions. The interband contribution does not seem effective in enhancing T_c for usual superconductors because the attractive region is too high in frequency, but it may be possible to find a material (or a system of materials) in which this mechanism could enhance or cause superconductivity under proper conditions.

Hence, as discussed above, demons can contribute to the enhancement of T_c, but the enhancement is effective only for s electrons which are relatively unimportant for conventional d band superconductors (that is, for high-T_c transition metals). The effects on the d electrons are only secondary, for example, through enhanced screening or through coupling to s electrons. Even if we achieve a negative μ^* for one type of electrons (s electrons) under special conditions, it is unlikely that this will result in a negative μ^* for the other type of electrons (d electrons), and the T_c of the whole system would be drastically reduced or destroyed by scattering unless the sample is extremely pure. We also note that a negative μ^* requires large mass ratios where, for some systems, localization and correlation effects render some of our approximations inappropriate. Because of the approximations involved, we do not regard the present calculation as conclusive for the existence of superconductivity with electron interactions alone. However, the calculations do suggest that it is not likely that the demon mechanism plays a dominant role or enhances T_c appreciably in conventional high-T_c transition metals (or compounds). As we have emphasized, the s and d electrons in our model were chosen to generally represent light and heavy electrons, and there may be better systems than transition metals to consider. For example, the components could be $s(p)$ and f electrons (even d and f electrons), two different carriers in semiconductors, etc.

ACKNOWLEDGMENTS

We acknowledge useful communications with Dr. J. W. Garland and Dr. W. F. Brinkman. This work was supported by the National Science Foundation Grant No. DMR7822465, Division of Materials Sciences, Office of Basic Energy Sciences, U.S. Department of Energy Grant No. W-7405-ENG-48, and Department of Energy Contract No. DE-AC03-76-ER00511.

*Present address: Dept. of Physics, Massachusetts Institute of Technology, Cambridge, Mass. 02139.

[1]A. A. Abrikosov, JETP Lett. 27, 33 (1978).
[2]M. L. Cohen, Phys. Rev. B 20, 1022 (1979).
[3]M. L. Cohen, in *Superconductivity in d- and f-Band Metals,* edited by H. Suhl and M. B. Maple (Academic, New York, 1980), p. 13.
[4]A. K. Rajagopal, Phys. Rev. B 20, 1020 (1979).
[5]D. Pines, Can. J. Phys. 34, 1379 (1956).
[6]J. W. Garland, in *Proceedings of the Eighth International Conference on Low Temperature Physics,* edited by R. O. Davies (Butterworths, Massachusetts, 1963), p. 143.
[7]V. Radhakrishnan, Phys. Lett. 16, 247 (1965).
[8]H. Fröhlich, J. Phys. C 1, 544 (1968).
[9]A. Rothwart, Phys. Rev. B 2, 3560 (1970).
[10]B. N. Ganguly and R. F. Wood, Phys. Rev. Lett. 28, 681 (1972).
[11]K. L. Kliewer and R. Fuchs, Phys. Rev. 181, 552 (1969).
[12]J. Ruvalds and L. M. Kahn, J. Phys. C 6, 460 (1978); I. Tüttö and J. Ruvalds, Phys. Rev. B 19, 5641 (1979); L. M. Kahn and J. Ruvalds, *ibid.* 19, 5652 (1979); I. Tüttö, L. M. Kahn, and J. Ruvalds, *ibid.* 20, 952 (1979); J. Ruvalds and C. M. Soukoulis, Phys. Rev. Lett. 43, 1263 (1979).
[13]J. W. Garland (private communication).
[14]P. W. Anderson, J. Phys. Chem. Solids 11, 26 (1959).
[15]*Superconductivity in d- and f-Band Metals,* edited by D. H. Douglass (AIP, New York, 1972).
[16]*Superconductivity in d- and f-Band Metals,* edited by D. H. Douglass (Plenum, New York, 1976).
[17]J. Bardeen, L. N. Cooper, and J. R. Schrieffer, Phys. Rev.

108, 1175 (1957).
[18]H. Ehrenreich and M. H. Cohen, Phys. Rev. 115, 786 (1959).
[19]J. Lindhard, K. Dan. Vidensk. Selsk. Mat.-Fys. Medd. 28, 8 (1954).
[20]M. L. Cohen, Phys. Rev. 134, A511 (1964). The definition of K_c in this paper is increased by a factor of 2 here to be consistent with the standard definition of μ^*.
[21]S. Doniach, in Proceedings of the Manchester Many Body Conference, 1964 (unpublished).
[22]N. F. Berk, Ph.D. thesis (University of Pennsylvania, 1966) (unpublished).
[23]S. Doniach and S. Engelsberg, Phys. Rev. Lett. 17, 750 (1966).
[24]J. R. Schrieffer, J. Appl. Phys. 39, 642 (1968).
[25]S. Doniach and E. H. Sondheimer, *Green's Functions for Solid State Physicists* (Benjamin, Massachusetts, 1974), p. 164.